Synthesis, characterization, and DFT study of novel metallo phtalocyanines with four carboranyl clusters as photosensitisers for the photodynamic therapy of breast cancer cells

Sevil Şener, A. Tahir Bayraç, B. Bilgenur Şener, Cem Tozlu, Nursel Acar, Bekir Salih, Mithat Yüksel, Özer Bekaroğlu

PII: S0928-0987(18)30552-9
DOI: https://doi.org/10.1016/j.ejps.2018.12.017
Reference: PHASCI 4789

To appear in: *European Journal of Pharmaceutical Sciences*

Received date: 1 October 2018
Revised date: 3 December 2018
Accepted date: 24 December 2018

Please cite this article as: Sevil Şener, A. Tahir Bayraç, B. Bilgenur Şener, Cem Tozlu, Nursel Acar, Bekir Salih, Mithat Yüksel, Özer Bekaroğlu , Synthesis, characterization, and DFT study of novel metallo phtalocyanines with four carboranyl clusters as photosensitisers for the photodynamic therapy of breast cancer cells. Phasci (2019), https://doi.org/10.1016/j.ejps.2018.12.017

Synthesis, characterization, and DFT study of novel metallo phtalocyanines with four carboranyl clusters as photosensitisers for the photodynamic therapy of breast cancer cells

Sevil Şener[a], A. Tahir Bayraç[b], B.Bilgenur Şener[b], Cem Tozlu[c], Nursel Acar[d], Bekir Salih[e], Mithat Yüksel [f], Özer Bekaroğlu[g*]*

[a]*Ege University, Aliaga Vocational School, 35800, İzmir-Turkey. E-mail:sevil.sener@ege.edu.tr*

[b]*Karamanoglu Mehmetbey University, Engineering Faculty, Bioengineering Department, 70100, Karaman, Turkey. E-mail:bayrac@kmu.edu.tr*

[c]*Karamanoglu Mehmetbey University, Engineering Faculty, Energy System Engineering Department, 70100, Karaman, Turkey. E-mail:bilgenurkandemir@kmu.edu.tr*

[d]*Ege University, Faculty of Science, Department of Chemistry, 35100 İzmir, Turkey. E-mail:nursel.acar@ege.edu.tr*

[e]*Hacettepe University, Chemistry Department, 06800, Ankara, Turkey. E-mail:bekir@hacettepe.edu.tr*

[f]*Ege University Department of Chemical Engineering, 35100, İzmir, Turkey. E-mail: mithat.yuksel@ege.edu.tr*

[g]*Faculty of Pharmacy, Istinye- University, Istanbul, 34010, İstanbul, Turkey. E-mail:obek@itu.edu.tr*

Corresponding authors:

e-mail: sevil.sener@ege.edu.tr

Tel: +90-232-6160671

Fax: +90-232-6161245

e-mail: obek@itu.edu.tr

Tel: +90-216-359013

Fax: +90-216-3860824

Abstract

The synthesis and characterization of novel Zn(II) and Co(II) phthalocyanines **4** and **5**, respectively containing four *o*-carboranyl units (40 boron atoms, 32.5% boron by weight) at the peripheral positions are described. The phthalocyanines (Pcs) were synthesized by cyclotetramerization of the previously prepared precursor 4-(2-thiol-*o*-carboranyl)thiolato-phthalonitrile **3** with the presence of metal salt in boiling dry DMF under a dry nitrogen atmosphere. They were characterized by elemental analysis, UV-Vis, FT-IR, MALDI-TOF mass and ^{1}H-NMR spectrometry. To elucidate the structural, spectroscopic and bonding properties of the obtained compounds, calculations with DFT/TD-DFT(Density Functional Theory/Time Dependent-Density Functional Theory) were performed. The cytotoxic effects of **4** and **5** on cancer cells and epithelial cells were determined. The targeted cytotoxicities of both compounds against cancer cells were analyzed with the cell viability test. Although, **4** caused less PDT (Photodynamic therapy) based decrease in cell viability of cancer cell line in comparison to **5**, it showed comparatively high cytotoxicity against cancer cells but not epithelial cells. The IC_{50} (half maximal inhibitory concentration) values indicate that **4** with PDT shows 17.3 fold more cytotoxicity to breast cancer cells than epithelial cells. The selectivity in cytotoxicity of **4** makes it a good candidate for cancer treatment. Interestingly, **5** was found to be highly cytotoxic for both cancer and epithelial cell lines. Considerably, **5** might be used as a cancer drug when combined with targeting agents such as antibodies and aptamers.

Keywords: Metallophthalocyanine, o-Carborane, Photodynamic therapy, Cytotox, Density Functional Theory.

1. Introduction

As a global problem, cancer is still fatal for a greater number of patients worldwide in spite of the progress in the basic research and therapy techniques. The mortality of cancer generally results from late diagnosis, inefficient therapies and tumor resistance to cancer drugs. Although a few drugs have very promising results, generally new generation cancer drugs and new clinical trials have culminated with only small progress in the treatment outcomes **[1,2].** There are a low number of new clinically approved drugs [**3]**. A group of cancer treatment modalities based on irradiation of photosensitizers (PS) has been explored and named as Photodynamic therapy (PDT). PDT is recognized as a minimally invasive and highly selective anticancer therapeutic technique **[4-7].** It consists of three essential components: photosensitizer (PS), light and oxygen **[8,9].** Phtalocyanines (Pcs) are administered in body via the oral or intravenous route and once they are photoexcited, reactive oxygen species (ROS) are generated and this causes an irreversible damage to cancer tissue **[10].** Among the PDT photosensitizers, porphyrin derivatives and organic dyes from the family of Pcs have gained a great deal of interest **[11,12].** Zinc phthalocyanine (ZnPc) which exhibits high photo- and chemical stability as required by chemical modifications as well as in vitro and in vivo applications, is a promising class of photosensitizers for PDT **[13-18]** due to its relatively high Photodynamic efficacy and high molar absorption coefficient ($\varepsilon \sim 10^5$ $M^{-1}cm^{-1}$) in the red part of the spectrum (ca. 630-730 nm), which allows increased tissue penetration of the activating light **[19].** Interestingly, owing to their extended flat hydrophobic aromatic surface, these macrocycles can interact with each other by attractive π–π stacking interactions **[20]**, leading to aggregation in solution.

Upon irradiation, ZnPc generates ROS within the range of 650-900 nm that leads penetration through target tissue **[21-24].** Various ligands, antibodies and drug carrier systems are used to provide selectivity of them in order to improve effectiveness and on the other

hand, decrease cytotoxicity against non-target tissue **[25-27].** Hence, there has been a growing interest in the synthesis of metallophtholocyanines (MPcs) carrying carboranyl units as models to develop radiosensitizers due to their selectivity of accumulation in tumor over many normal tissues to target tumoral tissue in boron neutron capture therapy (BNCT) treatment **[28]**. For the treatment of tumors by means of a combination of BNCT and PDT **[29]** have reported that two tetrasubstituted ZnPc bearing four carboranyl units have good photosensitizing efficiency. Recently, the enhancement of the Photodynamic efficacy of ZnPc has been achieved by conjugation of ZnPc with different numbers of lysine residues **[30].** In addition, the low toxicity of Pcs makes these dyes very promising agents for PDT applications as photosensitizers [**31]**. In the past decade, new materials involving carbon substituted carboranes have been used in theoretical studies **[32],** preparation of organic and organometallic compounds for the production of polymeric materials **[33,34],** and biological and medicinal research **[35].** These compounds have been proved to be useful in BNCT for cancer therapy **[36-39].**

Due to their potential use, polyhedral heteroboranes have been investigated intensively for more than 40 years. One of the subgroups of these compounds is dicarbo-*closo*-dodecaboranes, generally known as carboranes that have potential use in many different areas, especially in medicinal chemistry; BNCT **[29,40,41].** Carboranes are generally very stable toward heating as exemplified by *o*-carborane which remains unaffected up to 400 °C This makes *o*-carboranes very useful in biomedical applications.

It is the main objective of this paper to investigate the influence of the thio-*o*-carboranyl substituents on the photochemical properties of the phthalocyanines mentioned above. This is a fundamental prerequisite if such compounds to be used for bimodal therapies of tumor.

We report on the synthesis, characterization and phototoxicity of two novel ZnPc and CoPc bearing four *o*-carboranyl units at peripheral positions (Fig. 2). Moreover, we carry out Density Functional Theory (DFT) and Time Dependent-Density Functional Theory (TD-DFT) studies to shed light on their structural and electronic properties. Furthermore, we report a comparative study of the cytotoxic effects of phthalocyanines **4** and **5** on MCF7 breast cancer cells HTB-22™ and HEK 293 human embryonic kidney cells as cancer and epithelial cells.

2. Materials and methods

2.1. Materials

Reagent grade quality reagents and solvents were used throughout all the measurements. Commercial 1,2-dithiol-*o*-carborane (**1**) and 4-nitrophthalonitrile (**2)** were used as received. All reactions were carried out under a dinitrogen atmosphere.

2.2. Characterization techniques

Microanalyses were performed using a CHNS-932 (LECO) Elemental Analyzer. The ^{1}H-NMR spectra were recorded on a Agilent-NMR-vnmrs 600 spectrometer or VARIAN-INNOVA-600 MHz. Chemical shift values for ^{1}H-NMR were referenced relative to $Si(CH_3)_4$. The UV-Vis spectra were recorded on a Perkin-Elmer lambda 35 spectrophotometer, with 1 cm quartz cuvettes at room temperature. The IR spectra were obtained as KBR pellets on a Perkin Elmer Spectrum FT-IR Spectrophotometer. Mass spectra were obtained on a Voyager-DE^{TM} PRO MALDI-TOF-MS (Applied Biosystems, USA) having a nitrogen UV-Laser. The mass spectra were acquired in linear mode at various laser shots between 50 and 100. MALDI matrix, DHB was prepared in THF:H_2O:DMSO mixture in 3:1:1 (v/v/v) ratio at a concentration of 5 mg/mL and trifluoroacetic acid (0.2%) added. MALDI samples were prepared by mixing a sample (1 mg/mL in THF:H_2O:DMSO in 3:1:1 (v/v/v) including 0.2% trifluoroacetic acid) and the matrix solution (1:10; v/v) in a 0.5 mL microtube. At the last step,

0.5 µL of the final solution was applied to the sample target and dried prior to mass spectrometric analysis.

MCF7 breast cancer cells HTB-22™ and HEK 293 human embryonic kidney cells (CRL- 1573™) were obtained from ATCC (USA). Dulbecco's Eagle Modified Medium (DMEM) and Roswell Park Memorial Institute (RPMI) 1640 medium were purchased from Merck (USA). Fetal Bovine Serum (FBS) and Trypsin-EDTA solution was purchased from Sigma (USA). Penicillin/Streptomycin and Gentamycin sulfate were purchased from BI (USA). DPBS was purchased from Gibco-Thermo Fisher (USA). Alamar blue cell viability reagent was purchased from Thermo Fisher Scientific (Waltham, USA). Spectrophotometric data for the cytotoxicity experiments were obtained using Thermo Scientific Multiskan GO Microplate Spectrophotometer.

2.3. Chemical synthesis

Synthesis[1-sulfide-4-phtalonitrile-2-thio-o-carborane] 3.

Finely ground anhydrous Cs_2CO_3 (1.0 g, 8.0 mmol) was added to the solution of **1** (0.2 g, 1.0 mmol) and 4-nitrophthalonitrile **2** (0.36 g, 2.0 mmol) in acetonitrile (ACN) (25 ml). This solution was refluxed at 80 °C for 72 h under dry N_2 atmosphere. The solution was cooled to room temperature before filtration to remove unreacted reagents and also impurities. The obtained crude product was finally precipitated by addition of petroleum ether. The precipitate was washed with petroleum ether. It is readily soluble in polar solvents as acetone, tetrahidrofuran (THF), dimethlysülfoxide (DMSO), dimethlyfuran. Yield: 0.26 g (78%). Mp. 114 °C; Anal. Calculated for $C_{10}H_{14}N_2S_2B_{10}$: C, 35.91; H, 4.22; N, 8.38%, found C, 34.8; H, 4.5; N, 8.3%. UV-Vis (DMSO): λ_{max}/nm (log ε): 261 (4.04), 305 (3.48); ^{1}H NMR (acetone-d_6) δ ppm): 7.62 (d, 1H, J = 8.7 Hz); 7.14 (s, 1H); 7.03 (d, 1H, J = 8.7 Hz); 6.13 (br s, 1H, SH). IR (KBr): ν_{max}/cm^{-1}, 3484 and 3380 (H2O), 3094 (Ar-CH), 2539 (Ar-

BH), 2334 (S-H), 2227 (Ar-C≡N), 1634, 1593, 1574, 1491 (Ar-C=C), 1346, 1113, 1260 (Ar-C-N), 1224, 863, 836 (S-H), 721 (C-S), 523. MALDI-TOF MS: *m*/*z* 335.17$[M + H]^+$.

Synthesis[2,10,16,24-tetrakis-(1-sulfide-2-thio-o-carboranyl) phthalocyaninato Zn(II)] 4.

A mixture of **3** (0.10 g, 0.30 mmol) and $Zn(AcO)_2{\cdot}2H_2O$ (0.02 g, 0.08 mmol) was dissolved in DMF under dry N_2 atmosphere, in a sealed glass tube. Then this was heated for 24 h at 155 °C. After cooling the mixture to room temperature, the green-dark product was obtained and purified by washing with plenty of hot DMF, THF, ethyl acatate, chloroform, ether, ethanol and water. Finally, it was dried in a vacuum oven at 105 °C. This compound is soluble in warm DMSO. Yield: 0.03g (28 %). Anal. Calculated for $C_{40}H_{56}N_8S_8B_{40}Zn{\cdot}2H_2O$: C, 33.38; H, 4.20; N, 7.79%, found C, 32.8 ; H, 4.30; N, 7.6%. UV-Vis (DMSO): λ_{max}/nm (log ε): 350 (4.32), 673 (3.80), 698 (3.89). ^{1}H NMR (dmso-d_6, δ, ppm, TMS): 8.27 (s, 4H, Ar-H); 7.93 (s, 8H, Ar-H); 6.38 (s, 8H, S-H). (KBr, ν_{max}/cm^{-1}): 3610, 3300-3200 (H_2O), 3192 (Ar-CH), 2529 (B-H), 1647 (Ar-C=N), 1599 (Ar-C=C), 1457 (Ar C-N), 1393, 1105 (Ar-C=N), 1066 (S-H); 826 (C-S). MALDI-TOF MS: *m*/*z* 1403.8 $[M + H]^+$

Synthesis [2,10,16,24-tetrakis-(1-sulfide-2-thio-o-carboranyl)phthalocyaninato Co(II)] 5.

This was synthesized in the same way as described for **4**, only with the exception of $Co(AcO)_2{\cdot}4H_2O$ was used instead. The obtained green-dark mixture was washed succesively with hot DMF, THF, ethyl acatate, chloroform, ethanol, water and ether. Finally, it was dried in a vacuum oven at 105 °C. This compound is soluble in warm DMSO. Yield: 0.02 g (22%). Anal. Calculated for $C_{40}H_{56}N_8S_8B_{40}Co{\cdot}4H_2O$: C, 32.71; H, 4.39; N, 7.63%, found C, 33.4; H, 4.2; N, 7.5%. UV-Vis (DMSO): λ_{max}/nm (log ε): 325 (5.38), 615 (4.9), 678(5.2)**.** IR (KBr), ν_{max}/cm^{-1}): 3620, 3192 (H_2O), 2988 (Ar-CH), 2541(B-H), 1601 (Ar-C=N), 1579 (Ar-C=C), 1442 (Ar-C-N), 1393, 1312, 1105 (Ar-C=N), 1066 (S-H); 832 (C-S). MALDI-TOF MS: *m*/*z* 1397.2 $[M + H]^+$.

2.4. Cell Culture

HEK 293 human embryonic kidney cells and MCF7 breast cancer cells were used as epithelial and cancer cell models, respectively. HEK 293 cells have been extensively used in cell biology research many years because of their reliable growth as an epithelial cell line. Also MCF 7 is the one of the first and mostly used breast cancer cell line as a cancer model. MCF 7 cells were grown in RPMI Media supplemented with 10% FBS, 1% Penicillin-Streptomycin, and 0.1% Gentamycin sulfate. HEK 293 cells were grown in complete DMEM supplemented with 10% FBS and 1% Penicillin-Streptomycin. All cells were cultured in a 25 cm^2 cell culture flask with humidified atmosphere and 5% CO_2 at 37 °C. For subculturing media of cultured monolayers at 80% Confluency were discarded. The cells were washed with DPBS, then detached from the polystyrene surface using 2 mL trypsin–EDTA solution and incubated in humidified CO_2 incubator for 5 min. In order to inhibit cell surface damage caused by a further trypsin reaction, the reaction was stopped with 6 mL complete culture medium. The suspended cells have been counted using Thoma cell counting chamber. The cells were diluted with complete medium to have approximately 10^6 cell/mL, and agitated intermittently in order to prevent precipitation. Then the suspended cells were taken and placed in a sterile reservoir. For experimental purposes, the cells were cultured in 96-well plates (100 µL of cell suspension per well). The cells were incubated for attachment for 6 h before the treatment.

2.5. Cell Viability Assay

Stock solutions of **4** and **5** were prepared in DMSO as 40mM, 20mM and 5mM for cell viability assay. Media containing increasing concentrations (25, 100 and 200 µM) of **4** and **5** were prepared by addition of 5 µL of 5 mM, 20 mM and 40 mM solutions of **4** and **5** into separate tubes containing 995 µL of fresh medium, respectively. Each solution was filtered using 0.2 µm sterile filter before use in cell culture. Two different cell lines (MCF7 and HEK 293) were seeded on 96 well plates (10000 cells/well) and incubated for 6 hours in a

CO_2 incubator at 37°C to enable attachment. Media of the cells were discarded and 100 µL of previously prepared fresh media containing **4** and **5** (in %0.5 DMSO) were added into each well with designated increasing concentrations (0, 25, 100 and 200 µM). Negative control wells (only cell and only media) contained 0.5% DMSO in order to eliminate the effect of DMSO. Also an experiment on the cytotoxicity of DMSO was carried with increasing concentrations of DMSO prior to selection of 0.5 % DMSO as a solvent in cytotoxicity experiments (Figure S8). The samples were prepared in two groups and in triple repeats. One of the groups was exposed to light irradiation (20 J/m2) at 37°C for 55 min and then incubated in the dark (95% humidified CO_2 incubator, at 37°C) for 17 hours. OAI Trisol (class AAA) solar simulator coupled with an AM1.5 filter was used as the light source and the amount of radiation with 20 J/m^2 was applied to cell in all light intensity before each application. The other group was incubated in the dark at 37°C for 18 hours directly after addition of the drugs. Alamar blue reagent was added into the wells (1:10, v/v) and spectrophotometric measurements were carried out at 570 nm and 600 nm. Cell viabilities of each sample were calculated and significant differences between different concentrations were detected with multivariate non parametric Kruskal Wallis analysis method, using SPSS 17.0. Since more than two samples (0, 25, 100 and 200 µM concentrations) were intended to be compared, a multivariate comparison test was required. Each sample had three replicates and since three data points were achieved for each sample a non parametric test was preferred for analysis, with no assumption of normal distribution. Kruskal wallis method satisfied these requirements. Mann Whitney U test, a non parametric test used to compare two sample means, was used for the detection of significant differences between the treatment methods (PDT (+) and PDT(-)). The results were evaluated at a 95% confidence interval and the level of significance was 0.05 ($p<0.05$). The IC_{50} values of both 4 and 5 with and without PDT were calculated using linear regression analysis.

2.6. DFT studies

Gaussian09 **[42]** and Gaussview5.0 **[43]** and Spartan08 **[44]** programs were used in the calculations. DFT **[45]** was used to optimize the ground state geometries. The hybrid DFT Becke's three-parameter nonlocal exchange functional **[46,47]**, with Lee-Yang-Parr correlation functional (B3LYP) **[48]** was used for DFT calculations with-6-31G(d,p) basis set. All optimized structures were verified as minima by frequency analysis. The calculations were repeated in DMSO and in water for the most stable structures obtained from gas phase calculations. The TD-DFT calculations were carried out with ωB97XD and B3LYP functionals using 6-31G(d,p) basis set with the ground-state geometries obtained from B3LYP/6-31G(d,p). First 60 singlet excited states were used in calculations. UV-Vis spectra and molecular orbital energies of the studied systems were illustrated using ground state geometries. Electrostatic potential values were mapped to obtain total electron density surface of molecules in gas phase and in DMSO. Polarizable Continuum Model (PCM) **[49]** was used in all DFT and TD-DFT calculations and the effects of solvent on the electronic transitions were investigated in DMSO and in water.

3. Results and discussions

The synthesis of the target Pcs, **4** and **5,** was shown in Scheme 1. The key precursor **3** was obtained with a high yield of 77% after work-up. The detailed synthesis procedures as well as the characterization data are presented in the Experimental Section. The characteristic ν(C≡N) stretching band at 2227 cm^{-1} shows obvious evidence for the nucleophilic displacement of the nitro group, thus the formation of the **3**. The IR spectrum displays the typical ν(B–H) absorption frequency at 2539 cm^{-1}, characteristic of *closo*-carboranes **[50,51].** The new broadband appeared at 2334 cm^{-1} is attributed to the S–H stretching vibration. The characteristically broad ^{1}H NMR signal of the polar S–H unit in the carborane cage appears at 6.14 ppm, which is highly deshielded compared to that of 1-methyl-2-thiol-1,2-dicarba-*closo*-

dodecarborane **[52]** (Fig. S1)**.** This is consistent with the DFT calculations which shows that S–H has a positive charge (*vide infra*). This observed deshielding may be due to the very high acidity of the carbrorane **[53]** and also intermolecular hydrogen bonding between the adjacent molecules and the NMR solvents used. The aromatic protons appear as a singlet and two doublets in the expected range with the right integral values. The coupling constants are in complete agreement with the structure. The MALDI-TOF MS spectrum (Fig. S2) confirmed the expected value of the protonated molecular ion at *m/z* 335.17 (calc. *m/z* 335.19).

Compound **3** was readily converted to the novel Pcs **4** and **5** via cyclotetramerization in anhydrous DMF with the corresponding metal salts $Zn(OAc)_2 \cdot 2.H_2O$ or $Co(OAc)_2.4.H_2O$, respectively as depicted in Scheme 1. All Pcs exhibit good solubility in warm DMSO. The first direct evidence for the synthesis of **4** and **5** is provided by the IR spectra which show the complete disappearance of the cyano stretching band at 2227 cm^{-1} which is presented in **3**. The IR spectra of **4** and **5** are almost identical, and are in good agreement with the proposed structures. The characteristic strong B–H stretching vibration appears at 2529 cm^{-1}, and compared well with that of **3**. In the IR spectra, the new broad bands in the range of 3190 and 3400 cm^{-1} correspond to intermolecular hydrogen bond resulting from O–H stretching vibrations which indicates that both **4** and **5** are highly hydrated in the solid state as revealed by the Microanalysis as well. The ^{1}H-NMR spectrum of **4** shows two signals in the aromatic region at 8.27 and 7.93 ppm in a 1:2 ratio in complete agreement with the structure as shown in Scheme 1, (Fig.S1). They appear as singlets due to a statistical mixture of the obtained phthalocyanines. The singlet at 6.38 ppm can be assigned to the S–H, which is more deshilded in comparison to that **3**, as expected. ^{1}H-NMR analysis of **5** was excluded due to its paramagnetic nature.

MALDI-MS spectra of the phthalocyanines **4** and **5** (Fig.S2 and S3, respectively) were only obtained in linear mode. From positive ion linear mode MALDI-MS spectra, it is clearly

noticed that the complexes are very pure and only protonated molecular ion signals were observed beside the very limited number of the low molecular weight signals because of the fragment ions or clusters resulted from MALDI matrix. The precursor **3** and the metal complexes of phthalocyanines **4** and **5** were observed in DHB (Dihyroxybenzoic acid) at higher intensities compared to the other MALDI matrices. These results showed that the corresponding metallophthalocyanines were synthesized in the desired manner.

The intermolecular interactions of dimeric molecules can lead to the formation of hydrogen bonds between the hydrogen atom of the polar group and isoindole nitrogen atom of neighboring one. This is mainly caused by aggregation of the Pc molecules in the solution **[50]**.

UV-Vis spectra of the new boronated phthalocyanines **4** and **5** in warm DMSO are presented in Fig.1. The spectra of both display characteristic absorptions of phthalocyanines, with Q-bands at between 698 and 678 nm, respectively, whereas the B-band absorptions were observed at around 370-250 nm.

Fig. 1.

In order to evaluate the electronic transitions, structures of the related systems should be known. The nature and types of electronic transitions merely depend on the structures. The optimized ground-state molecular structures of **4** and **5** are given in Fig. 2 in DMSO at B3LYP/6-31G(d,p) level. While carborane-SH groups are oriented up and down, Pcs keep their planar structure (the most stable conformer; Table S1, Fig. S4). These two directions from Pc have an approximate angle of 105º (C-S-C angle) in the gas phase and in DMSO.

Another important observation is the S-H…B distance which is measured as 2.86 Å and it indicates a nonclassical hydrogen bonding. The distances between S-H groups and indoles are around 4 Å and make the intramolecular charge transfer (ICT) easier.

Fig. 2.

Complexation energies for the investigated systems were calculated in gas phase and in solution according to the synthesis reactions in Scheme 1 and the stabilities of the formed complexes were determined. Table S2 shows dipole moments (μ, Debye), total electronic energies including zero point correction energies (E_{elec}+ZPE, Hartree), total electronic energies including free energy changes (E_{elec}+ΔG, Hartree), complexation energies (ΔE_C) and reaction free energies (ΔΔG) of studied compounds in the gas phase, in DMSO (ε = 46.826) and in water (ε = 78.355), calculated at B3LYP/6-31G(d,p) level. Stable complexes are characterized by negative complexation energies in gas phase and in solvents. **5** forms the most stable complexes in both media. The negative ΔΔG values observed in solvents indicate that the complexes are more easily formed in solution than the gas phase.

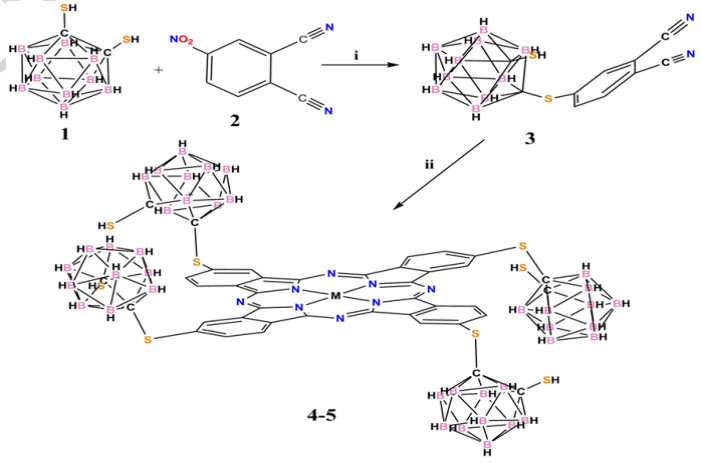

Scheme 1. Synthesis of **3**, **4 ZnPc** and **5 CoPc** (i) Cs_2CO_3, N_2, ACN, 80 ^{0}C, 72 h, (ii) or

$Zn(OAc)_2 \cdot 2H_2O$ or $Co(OAc)_2 \cdot 4H_2O$ 155 ^0C , DMF, N_2, 24 h.

Electron affinity and ionization potential are in correlation with lowest unoccupied molecular orbital (LUMO) and highest occupied molecular orbital (HOMO), respectively. Fig. S5 displays the HOMO-LUMO transition energies for the complexes in the gas phase and in DMSO. HOMO-LUMO levels and energy gaps, ΔE_{H-L} are also given for comparison. Because of the unoccupied single electron of Co(II), single occupied molecular orbital (SOMO) was shown for compound **5**.

HOMO and LUMO energies of all studied molecules have very small negative values in gas phase and in solvents both with ωB97XD/6-31G(d,p) and B3LYP/6-31G(d,p) levels. Lower energy gaps enable intramolecular charge transfer much more easily by supporting intramolecular charge transfer interactions (*vide supra*, electronic UV-Vis discussion). HOMO and LUMO are located on the conjugated rings of MPcs (Fig. S5). HOMO-LUMO energy gap of **4** is smaller than that of **5** in gas phase and in solvents with both methods. SOMO-LUMO energy gap for **5** has the highest value as 5.31 eV in the same level in DMSO. Thus, **4**, able to make a charge much easier, is more suitable than **5** for charge transfer systems.

Optimized ground state geometries were used to calculate the excitation energies and absorption wavelengths of all studied systems from S_0 to S_{60} states using TD-DFT at ωB97XD/6-31G(d,p) level. Selected electronic transitions are discussed in Table S3 using the highest occupied and the unoccupied molecular orbitals in DMSO (Fig. S6).

$S_0 \rightarrow S_1$ transition with high oscillator strength (655 nm in DMSO) has $\pi \rightarrow \pi^*$ character between HOMO and LUMO orbitals at ωB97XD/6-31G(d,p) level. This peak was calculated as 623 nm in DMSO at B3LYP/6-31G(d,p) level. The experimental UV-Vis data also show a peak at 697 nm, Q-band for Pcs (Fig.1). The ωB97XD values are in better agreement with the

experimental values in DMSO; therefore, the following discussion is based on ωB97XD/6-31G(d,p) results unless otherwise stated.

Metal-to-ligand charge transfer (MLCT) peak appeared in $S_0 \rightarrow S_3$ transition (374 nm) between HOMO-2 and LUMO in DMSO (Fig. 3). Because of very low oscillator strength, this peak was not observed in experimental spectra. Additionally, charge transfer from S atom (between carborane and Pc) to Pc (ICT1) and local excitation of Pc (LE) have also contribution at this transition. $S_0 \rightarrow S_4$ transition has also similar characteristics with low oscillator strength between HOMO-2 and LUMO+1 orbitals. A third intramolecular charge transfer from S-H in carborane groups and phenyl groups to Pc core (ICT2) was observed with low contribution between 316-331 nm in DMSO. Local excitaion of Pc (LE) became again more significant with high oscillator strength at 299 nm (B-band). Before B-band (between 200-300 nm) additional charge transfers are observed: intramolecular charge transfer from Pc to C-S (ICT3), from Pc to carborane (ICT4, 213-317 nm) and finally from carborane to Pc (ICT5, 211 nm). Computational UV-Vis spectrum calculated in water displays similar properties (Fig. 3)

The UV-vis absorption spectra of phthalocyanines show the characteristic absorptions of monomolecular phthalocyanines in solution, with Q-band (π-π*) at 650-700 nm and a Soret-band (B-band) around 300-400 nm Fig.1. B-band is less intense and broader π-π* transition for Phthalocyanines. B-band was affected by the modification of carborane groups and single-bond S-H of Pc. n-σ* ve n-π* transitions from non-bonding electrons in S in carborane and S between phenyl and carborane could increase the strength of B band. Therefore, the carborane modification does influence the absorption behaviour. This situation has been proved by the computational study which shows electron moves from S-H groups to Pc. Experimental UV data also showed two peaks at 678 nm, and 325 nm Fig.1 for **5**. The calculated UV-Vis absorption spectra of 5 was not well resolved for all transitions. The

wavelength range of solar simulator spectra is from 400 nm to 1100 nm. Q-band (π-π*) of phthalociyanine molecule in absorption spectra is well matched with spectral range of light source. B-band (300 nm – 400 nm) of phthalocyanine molecule remains out of range of light wavelength. Therefore, π-π* electronic transitions in Q-band of phthalocyanine molecule is dominant in cell viability assay.

Fig. S7 illustrates the total electron densities for the investigated systems in the gas phase and in solution. The electrostatic potential surface is used to map total electron densities. The colors represent the quantity of the electron density: red, electron rich, partialy negative charge; yellow, slightly electron rich region; green, neutral; light blue, slightly electron deficient; blue, electron deficient, partialy positive charge. The electron density was calculated using the Mulliken charge distribution. The maximum and minimum ranges of the total electron density values for the used colors are also given in Fig. S7 In **4**, the positive electrostatic potential (blue area) is localized around the Zn atom in the middle ring. S-H substituent has a positive charge. Carborane carries slightly negative charges.

Fig. 3.

Total electron distribution revealed that electrons are mostly localized away from zinc and S-H on carborane both in gas phase, in DMSO and in water. The distribution is increased in water. Carborane has slightly negative charge. These distributions and the calculated results show that –SH groups on carborane moiety may be responsible for π-π* transitions and n-π* transitions.

Fig. 4.

After 18 h incubation with Pcs with and without PDT, cell viabilities of HEK 293 and MCF 7 cells were analyzed by cytotoxicity test in Fig.4. Both cell lines and the Pcs show different viability profiles with the same therapy conditions. Without PDT, **4** (200 μM) decreased the cell viability of MCF 7 to 66.7±4.3% but HEK 293 to 90.1±4.8%. Upon application of PDT to **4** cell viabilities of MCF 7 and HEK 293 was 35.2±2.7% and 89.3±5.3%, respectively. This shows that **4** has selectively and significantly higher toxicity to cancer cells than epithelial cells with and without PDT. Also PDT increases the cytotoxicity of **4** further 31% causing more cells to undergo apoptosis.

Phthalocyanine **5** shows more dramatic effects on both cell lines and showed higher toxicity in each condition applied. Without PDT, **5** (200 μM) decreased the viability of MCF 7 to 20.6±4.3 and HEK 293 to 47.2±2.8. When PDT applied with **5,** viability of both cell lines was lower than 9%. This result shows us that **5** is not selective as **4** on the cancer cells and causes toxicity to both cell lines. Both **5** and **4** show higher toxicities with increasing the concentrations. Also PDT increases the toxicity in each case and the concentration. This shows that both photosensitizers are suitable for PDT but selectivity of **4** on the cancer cell line makes it a better candidate.

The IC_{50} values show that **4** is 3.7 fold more cytotoxic for breast cancer cells than for the epithelial cells Table 3. On the other hand, although **5** is more cytotoxic for both cell lines, the IC_{50} values for two cell lines are closer. Upon PDT treatment, there was no significant difference in cytotoxicity of **4** for HEK 293 cells; but the cytotoxicity increased by further 4.5 fold for MCF 7 cells; which means PDT together with **4** treatments selectively affected the

viability of the breast cancer cells. Also, it is obvious that 17.3 fold increase in IC_{50} value of MCF 7 PDT(+) **4** when compared to HEK 293 PDT (+) **4** shows its effectiveness. PDT treatment applied with **5** treatment showed approximate cytotoxicity for both cell lines.

Table 3. IC_{50} values of **4** and **5** treatments with (PDT(+)) and without (PDT(-)) PDT for MCF7 and HEK293 cells

	MCF 7		**HEK 293**	
	PDT(+)	**PDT(-)**	**PDT(+)**	**PDT(-)**
4	74.55	337.82	1290.48	1248.59
5	81.55	90.04	81.58	166.31

Kruskal Wallis data showed that there was no significant difference between 0, 25, 100 and 200 µM concentrations of **4** with and without PDT ($p>0.05$), proving that the treatment has no cytotoxic effect on HEK 293 epithelial cells (Table 4). All other treatments were significantly affected the viability of the cells in a dose dependent manner ($p<0.05$).

Table 4. Kruskal Wallis method was used to detect concentration dependent significant differences of drugs with and without PDT treatment.

p values	**MCF 7**	**HEK 293**
4, PDT(-)	0.019	**0.118**
4, PDT(+)	0.016	**0.053**
5, PDT(-)	0.016	0.016
5, PDT(+)	0.016	0.016

Mann Whitney U test showed that MCF 7 viabilities vary significantly due to PDT when 4 was used in 100 µM and 200 µM, while there was no significant difference in HEK cell viabilities in all concentrations (Table 5). On the other hand, 5 showed significant difference in cell viabilities when PDT applied in 100 µM and 200 µM, regardless of cell type. Only for 25 µM, a selective decrease in MCF 7 viability could be seen.

Table 5. Mann Whitney U test was used to detect significant differences between cell viabilities of PDT (+) and PDT (-) therapies for each concentrations of **4** and **5**.

p values	MCF 7			HEK 293		
	25 µM	100 µM	200 µM	25 µM	100 µM	200 µM
4	0,275	**0,049**	**0,049**	0,827	0,513	0,513
5	**0,049**	**0,049**	**0,049**	0,127	**0,049**	**0,049**

The cytotoxic effects of **5** and **4** on the cancer cells and the epithelial cells were compared and cytotoxicities of these two compounds against the cancer cells were shown. While both compounds have cytotoxic effects on the cancer cells, compound **4** selectively decreased the viability of the cancer cells. When used in combination with PDT, the selectivity of **4** treatment increased. Besides **4** showing higher PDT based decrease in cell viability when compared to **5**, it also shows aselective increase in cytotoxicity against the cancer cells. This makes this compound a potential drug candidate. On the other hand, with its significant cytotoxicity, **5** could also be used as a drug in combination with targeting agents such as antibodies and aptamers. As an example, teraphthal, a catalytic sensitizer with a main component of cobalt phthalocyanine was shown to destroy tissues after adding ascorbic acid, and because of its ferromagnetic properties. It can also be used with magnetic liposomes in order to improve their magnetic properties **[54]**. Moreover, gold nanoparticles were used to avoid non-specific cytotoxic effects of metal free phthalocyanines and also increase their biocompatibility **[55]**. Modification of photosensitizer with thiol tether enables photosensitizers to attach on the surface of gold nanoparticles and makes them dissolve in polar solvents while keeping their hydrophobic character which is essential for tumour targeting and PDT efficacy **[56]**.

4. Conclusions

In the present work, we report syntheses of novel type of phthalocyanines with *o*-carboranyl units. Their structural and electronic properties have been studied in details by experimental techniques, such as CHN, UV–Vis, FT-IR, ^{1}H NMR, and MALDI-TOF mass spectroscopy, and also by DFT and TD-DFT methods in gas phase, in DMSO and in water.

The calculated data are in good agreement with the experimental results. The cell viability tests have shown that these compounds **4** and **5** have a marked cytotoxicity against the cancer cells used; which make them very promising agents for cancer therapy.

Acknowledgements

We gratefully acknowledge the financial support from Şerife Şener Öcal. We also thank computer time on FenCluster provided by Ege University Faculty of Science and TUBITAK-ULAKBIM Truba Resources. Prof. Dr. Bekir Salih gratefully acknowledges the Turkish Academy of Sciences (TUBA) for the partial financial support. We gratefully acknowledge Prof. Dr. Abdurrahman Şengül, for his support during the study.

References

[1] J.Berg. J. Clin. Oncol. 27(2009) 2-5. doi: 10.1200/JCO.2008.18.8342

[2]T. Fojo , C. Grady. J. Nat. Cancer Inst. 101(2009)1044-1048. doi:/10.1093/jnci/djp177

[3] T.Hampton. JAMA 296 (2006) 1951-1952. doi:10.1001/jama.296.16.1951

[4] P. Agostinis, K. Berg, K.A. Cengel, T.H. Foster, A. W. Girotti, S.O. Golinick, S.M. Hahn, M.R. Hamblin, A. Juzeniene, D. Kessel, M. Korbelik, J. Mohan, P. Mroz, D. Nowis, J. Piette, B.C. Wilson. CA: A Cancer Journal for Clinician 61 (2011) 250-281. doi:10.3322/caac.20114

[5] R.R. Allison, C.H. Sibata. Photodiagnosis Photodyn. Ther. 7 (2010) 61-75. doi:10.1016/j.pdpdt.2010.02.001

[6] B.Chen, T. Roskams, P.A.M. de Witte. Photochem. Photobiol. 76 (2002) 509-513. doi:10.1562/0031-8655(2002)076%3C0509:ATEBHM%3E2.0.CO;2

[7] D. Grose, W. Anseline , P. Smıth. Dermatologic Surgery 40 (2014) 1441-1442. doi: 10.1097/DSS.0000000000000187

[8] T.J. Dougherty, C.J. Gomer, B. Henderson, G. Jori, D. Kessel, M. Korbelik, J. Moan , Q. Peng. J. Nat Cancer Inst. 90 (1998) 889-905. doi:10.1093/jnci/90.12.889

[9] D.E.J.G.J. Dolmans, D.Fukumura, R.K. Jain. Nat. Rev. Cancer 3 (2003) 3380-387. doi:10.1038/nrc1071

[10] R. Tong, H. Lin, Y. Chen, N. An, G. Wang, X. Pan, F. Qu. Mat. Sci. Engi:C 78 (2017) 998-1005. doi:10.1016/j.msec.2017.04.112

[11] D. Flak, L. Yate, G. Nowaczyk, S. Jurga. Mat. Sci. Engi:C 78 (2017) 1072-1085. doi:10.1016/j.msec.2017.04.107

[12] M. Ascencio, P. Collinet, M.O. Farine, S. Mordon. Lasers Surg. Med. 40 (2008) 332-341. doi:10.1002/lsm.20629

[13] J.Y. Liu, P.C. Lo, W.P. Fong, D.K. Ng. Org. Biomol. Chem. 7 (2009) 1583−1591. doi:10.1039/B822128F

[14] J.Y. Liu, X.J. Jiang, W.P. Fong, D.K. Ng. Org. Biomol. Chem. 6 (2008) 4560−4566. doi:10.1039/B814627F

[15] L.N. Milla, E.I. Yslas, A. Cabral, E.N. Durantini, S. Romanini, V. Rivarola, M. Bertuzzi. Biomed. Pharmacotherapy 63 (2009) 209−215. doi:10.1016/j.biopha.2008.01.019

[16] W. Duan, P.C. Lo, L. Duan, W.P. Fong, D.K. Ng. Bioorg. Med. Chem. 18 (2010) 2672−2677. doi:10.1016/j.bmc.2010.02.020

[17] A.H.A. Machado, K.C.M. Moraes, C.P. Soares, M.B. Junior, N.S. da Silva. Photomed. Laser Surg. 28 (2010) 143−149. doi:10.1089/pho.2009.2561

[18] M. Bai, P.C. Lo, J. Ye , C. Wu, W.P. Fong, D.K. Ng. Org. Biomol. Chem. 9 (2011)

7028−7032. doi:10.1039/C1OB05955F

[19] A. Zielichowska, J. Saczko, A. Garbiec, M. Dubinska-Magiera, J. Rossowska, P. Surowiak, A. Choromanska, M. Daczewska, J. Kulbacka J, H. Lage. Biomed. Pharmacotherapy 69 (2015)145–152. doi:10.1016/j.biopha.2014.11.017

[20] C.A. Hunter, J. K. M. Sanders. J. Am. Chem. Soc. 112 (1990) 5525-5534. doi: 10.1021/ja00170a016

[21] R. Bonnett. Chem. Soc. Rev. 24 (1995) 19-33. doi: 10.1039/CS9952400019

[22] M.P. De Filippis, D. Dei, L. Fantetti, G. Roncucci. Tetrahedron Lett. 41 (2000) 9143-9147. doi:10.1016/S0040-4039(00)01638-5

[23] C. Fabris, G. Valduga, G. Miotto, L. Borsetto, G. Jori, S. Garbisa, E. Reddi. Cancer Research 61 (2001) 7495-7500. doi: Published October 2001

[24] J. Bogdan, J. Pławińska-Czarnak, J. Zarzyńska. Nanoscale Research Lett. 12 (2017) 225. doi:10.1186/s11671-017-2007-y

[25] S.A. Sibani, P.A. McCarron, A.D. Woolfson, R.F. Donnelly. Expert Opin Drug Deliv. 5 (2008) 1241-1254. doi:10.1517/17425240802444673

[26] W. Chen, J. Ouyang, H. Liu, M. Chen, K. Zeng, J. Sheng, Z. Liu, Y. Han, L. Wang, L. Deng, L. You-Nian, S. Guo. Advanced Materials 29 (2017) 1603864. doi: 10.1002/adma.201603864

[27] T. Stuchinskaya , M. Moreno, M.J. Cook, D.R. Edwards, D.A. Russell. Photochem Photobiol Sci 10 (2011) 822-831. doi:10.1039/C1PP05014A

[28] V.I. Bregadze, I.B. Sivaev, D. Gabel, D. Whorle. J. Porphyrins Phthalocyanines 5 (2001)

767–781. doi:10.1002/jpp.544

[29] F. Giuntini, Y. Raoul, D. Dei, M. Municchi, G. Chiti, C. Fabris, P. Colautti, G. Jori, G.Roncucci. Tetrahedron Lett. 46 (2005) 2979–2982. https://doi.org/10.1016/j.tetlet.2005.03.030

[30] L. Li, Z. Luo, Z. Chen, J. Chen, S. Zhou, P. Xu, P. Hu, J. Wang, N. Chen, J. Huang, M. Huang. Bioconjugate Chem. 23 (2012) 2168−2172. doi: 10.1021/bc3002997

[31] L. Sobotta, M. Wierzchowski, M. Mierzwicki, Z. Gdaniec, J. Mielcarek, L. Persoons, T. Goslinski, J. Balzarini. J. Inorg. Biochem. 155 (2016) 76–81. doi:10.1016/j.jinorgbio.2015.11.006

[32] S.H. Wu, M. Jr Jones. J. Am. Chem. Soc. 111 (1989) 5373-5384. doi: 10.1021/ja00196a049

[33] N. Mayes, J. Greene, M.S. Cohen. J. Polymer Sci. Part A 5 (1967) 365-379. doi:10.1002/pol.1967.150050212

[34] D. Brown, H.M. Colquhoun, J.A. Daniels, J.A.H. MacBride, I.R. Stephenson, K. Wade. J. Materials Chem. 2 (1992) 793-804. doi: 10.1039/JM9920200793

[35] R.J. Paxton, B.G. Beatty, M.F. Hawthorne, A. Varadarajan, L.E. Williams, F.L. Curtis, C.B. Knobler, J.E. Shively. Proc. Nat. Acad. Sci. USA 88 (1991) 3387-3391. doi:10.1073/pnas.88.8.3387

[36] R.F. Barth, A.H. Soloway, R.G. Fairchild. Cancer Research 50 (1990) 1061-1070.

[37] K. Shelly, D.A. Feakes, M.F. Hawthorne, P.G. Schmidt, T.A. Krish, W.F. Bauer. Proc. Nat. Acad Sci. USA 89 (1992) 9039-9043. doi:10.1073/pnas.89.19.9039.

[38] M.F. Hawthorne. Pure & Appl Chem. 63 (1991) 327-334. doi:10.1351/pac199163030327.

[39] M.F. Hawthorne. Angew Chem. Int. 32 (1993) 950-984. doi:10.1002/anie.199309501

[40] M.F. Hawthorne, A. Maderna. Chem. Rev. 99 (1999) 3421-3434. **doi:**10.1021/cr980442h

[41] R. Luguya, T.J. Jensen, K.M. Smith, M.G.H. Vicente. Bioorg. Medicinal Chem. 14 (2006) 5890-5897. doi:10.1016/j.bmc.2006.05.026

[42] M.J. Frisch, G.W. Trucks, H.B. Schlegel, G.E. Scuseria, M.A. Robb, J.R. Cheeseman, G. Scalmani, V. Barone, B. Mennucci, G.A. Petersson, H. Nakatsuji, M. Caricato, X. Li, H.P. Hratchian, A.F. Izmaylov, J. Bloino, G. Zheng, J.L. Sonnenberg, M. Hada, M. Ehara, K. Toyota , R. Fukuda, J. Hasegawa, M. Ishida, T. Nakajima, Y. Honda, O. Kitao, H. Nakai, T . Vreven, J.A. Montgomery, J.E. Peralta, F. Ogliaro, M. Bearpark, J.J. Heyd, E. Brothers, K.N. Kudin, V.N. Staroverov, R. Kobayashi, J. Normand, K. Raghavachari, A. Rendell, J.C. Burant, S.S. Iyengar, J. Tomasi , M. Cossi, N. Rega, J. M. Millam, M. Klene, J. E. Knox, J. B. Cross, V. Bakken, C. Adamo, J. Jaramillo, R. Gomperts, R. E. Stratmann, O. Yazyev, A. J. Austin, R. Cammi, C. Pomelli, J. W. Ochterski, R. L. Martin, K. Morokuma, V. G. Zakrzewski, G. A. Voth, P. Salvador, J. J. Dannenberg, S. Dapprich, A. D. Daniels, Ö. Farkas, J. B. Foresman, J. V. Ortiz, J. Cioslowski, D. J. Fox. Gaussian, Inc., Wallingford CT, 2009.

[43] R. Dennington, T. Keith, J. Millam, GaussView 5.0.9 Semichem Inc., Shawnee Mission K.S. (2009).

[44] Spartan08 for Windows, Wavefunction, Inc. Irvine, CA 92612 USA.

[45] W. Kohn, L. J. Sham. Phys. Rev. **140** (1965) A1133-A1138. doi: 10.1103/PhysRev.140.A1133

[46] A.D. Becke. Phys Rev. A, **38** (1988) 3098-3100. doi: 10.1103/PhysRevA.38.3098.

[47] A.D. Becke. J. Chem. Phys. **98** (1993) 5648-5652. doi:10.1063/1.464913

[48] C. Lee, W. Yang, R.G. Parr. Phys. Rev. B **37** (1988) 785-789. doi:10.1103/PhysRevB.37.785

[49] J. Tomasi, B. Mennucci, E. Cancès. J. Mol. Struct. THEOCHEM. **464** (1999) 211-226. doi:10.1016/S0166-1280(98)00553-3

[50] A. Laromaine, F. Teixidor, R. Kivekäs, R. Sillanpää, R. Benakki, B. Grüner, C. Viñas. Dalton Trans. 10 (2005) 1785-1795. doi: 10.1039/B502328A

[51] D. Wöhrle, O. Tsaryova, A. Semioshkin, D. Gabel, O. Suvorova. J. Organomet. Chem. 747 (2013) 98-105. doi:10.1016/j.jorganchem.2013.03.020

[52] F. Teixidor, J. Rius, C.Miravitlles, C. Vinas, L. I. Escriche, E. Sanchez, J. Casabo. Inorg. Chim. Acta 176 (1990) 61-65. doi:10.1016/S0020-1693(00)85092-6.

[53] J. Plešek, S. Heřmánek. Chem. Commun. 44 (1979) 24-33. doi:org/10.1135/cccc19790024

[54] A.R. Harutyunyan, A. A. Kuznetsov, O.A. Kuznetsov, O.L. Kaliya. J. Magnetism Magnetic Materials 194 (1999) 16-21. doi:10.1016/S0304-8853(98)00576-9

[55] S.M.I. Alexeree, M.A. Sliem, R.M. EL-Balshy, R.M. Amin RM, M.A. Harith. Materials Sci. Engi: C 76 (2017) 727-734. doi:10.1016/j.msec.2017.03.129

[56] D.C. Hone, P. I. Walker, R. Evans-Gowing, S. FitzGerald, A. Beeby, I. Chambrier, M. J. Cook, D.A. Russell. Langmuir 18 (2002) 2985-2987. **doi:** 10.1021/la0256230

Figure Caption

Fig. 1. UV-Vis absorption spectra of **3** (blue line), **4** (black line) and **5** (red line).

Fig. 2. Optimized structures of **4** and **5** in DMSO at B3LYP/6-31G(d,p) level.

Fig. 3. Calculated UV/Vis absorption spectra of **4** with oscillator strength values in DMSO and in water at ωB97XD/6-31G(d,p) level.

Fig. 4. Cell viabilities of **(a)** MCF 7 ($p<0.05$ for all four treatments), and **(b)** HEK 293 cells ($p>0.05$ for **4**, PDT(+) and PDT(-)) after incubation with **4** and **5**, with (PDT (+)) and without (PDT(-)) light irradiation.

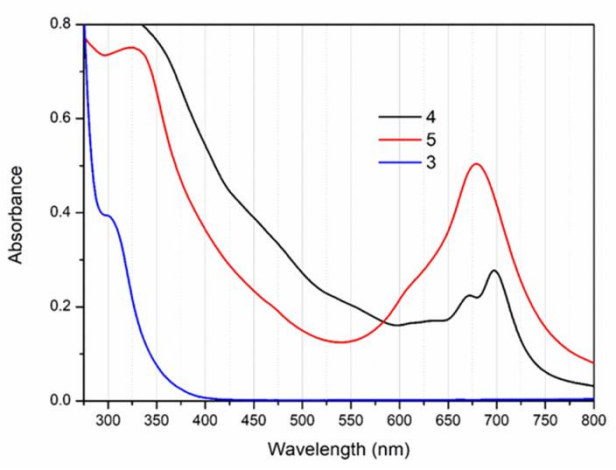

Fig. 1

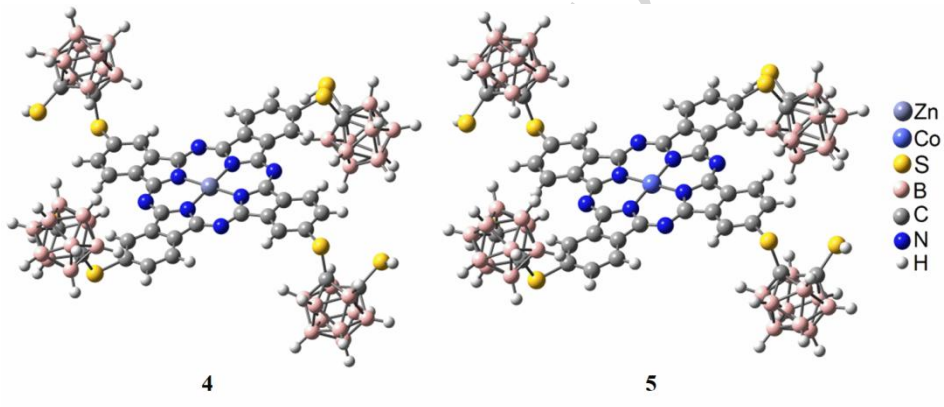

Fig. 2.

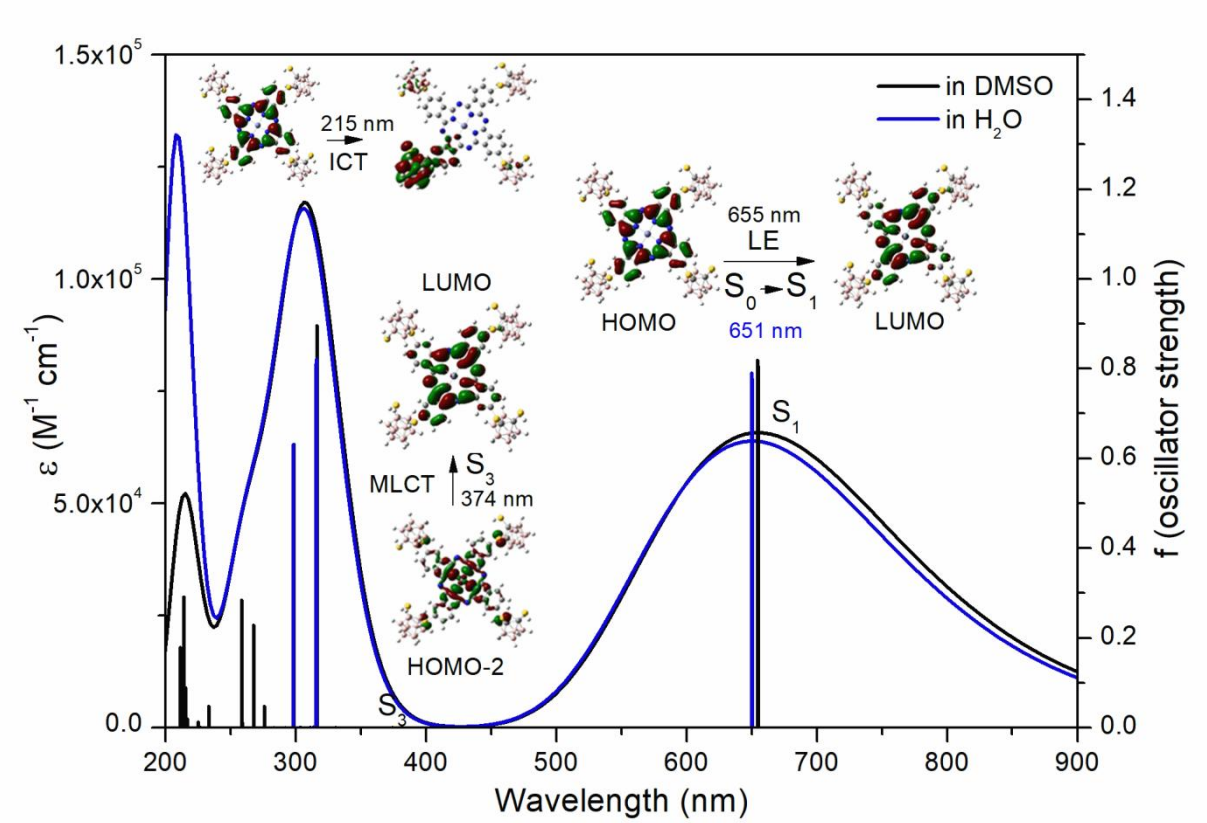
1.5x10^5
1.0x10^5
5.0x10^4
0.0
ε (M^-1 cm^-1)
f (oscillator strength)
1.4
1.2
1.0
0.8
0.6
0.4
0.2
0.0
200
300
400
500
600
700
800
900
Wavelength (nm)
in DMSO
in H2O
215 nm
ICT
LUMO
MLCT
S3
374 nm
HOMO-2
S3
655 nm
LE
S0 → S1
651 nm
HOMO
LUMO
S1

Fig. 3.

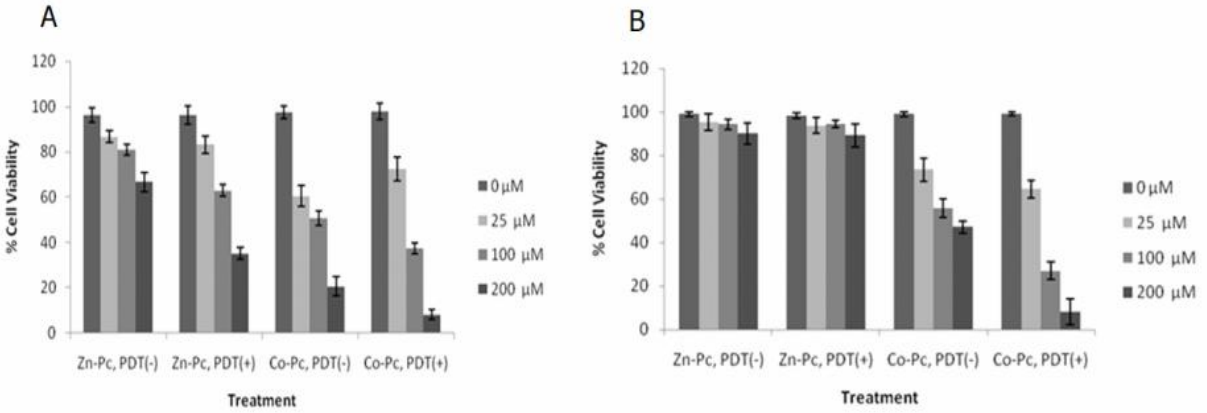
A
B
% Cell Viability
120
100
80
60
40
20
0
Zn-Pc, PDT(-)
Zn-Pc, PDT(+)
Co-Pc, PDT(-)
Co-Pc, PDT(+)
Treatment
0 µM
25 µM
100 µM
200 µM

Fig. 4.

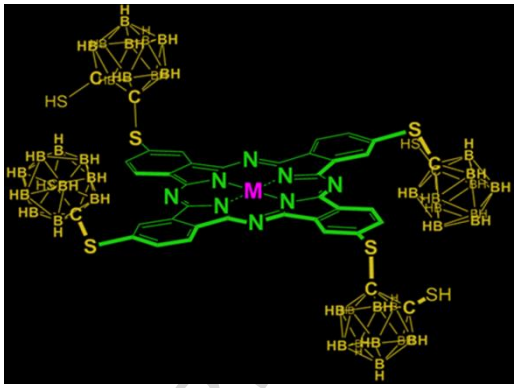

Graphical abstract